Supporting information

A tailor made deazaflavin-mediated recycling system for artificial nicotinamide cofactor biomimetics

Jeroen Drenth[†‡], *Guang Yang*[†‡], *Caroline E. Paul*[§] *and Marco W. Fraaije*[†*]

[†]Molecular Enzymology Group, University of Groningen, Nijenborgh 4, 9747AG Groningen, The Netherlands

[§]Department of Biotechnology, Delft University of Technology, Van der Maasweg 9, 2629HZ Delft, The Netherlands

[§]These authors contributed equally to this work

*Corresponding author: m.w.fraaije@rug.nl

Table of contents

QuikChange mutagenic primers used to engineer *Tfu*-FNO

Table S1: QuikChange mutagenic primers used to engineer *Tfu*-FNO. Abbreviations fw and rv are used to designate the forward and reverse primers, respectively. Primers were designed using the Agilent QuikChange primer design tool (www.genomics.agilent.com; primerDesignProgram.jsp).

Mutation		Primer sequence
A87S	fw	tcccacggaaccgacacgatcaccacg
	rv	cgtggtgatcgtgtcggttccgtggga
V113S	fw	gaaacccagcgggttcgaacagtcgacgacgatc
	rv	gatcgtcgtcgactgttcgaacccgctgggtttc
G29F	fw	gcggccctgatcaaacgtgccccccagc
	rv	gctggggggcacgtttgatcagggccgc
G29H	fw	gcggccctgatcatgcgtgccccccagc
	rv	gctggggggcacgcatgatcagggccgc
G29I	fw	gcggccctgatcaatcgtgccccccagc
	rv	gctggggggcacgattgatcagggccgc
G29L	fw	cgcggccctgatctagcgtgccccccagc
	rv	gctggggggcacgctagatcagggccgcg
G29M	fw	ccgcggccctgatccatcgtgccccccagca
	rv	tgctggggggcacgatggatcagggccgcgg
G29N	fw	gcggccctgatcattcgtgccccccagc
	rv	gctggggggcacgaatgatcagggccgc
G29Q	fw	cgcggccctgatcctgcgtgccccccagc
	rv	gctggggggcacgcaggatcagggccgcg
G29S	fw	ggccctgatcactcgtgccccccag
	rv	ctggggggcacgagtgatcagggcc
G29V	fw	ggccctgatcaaccgtgcccccc
	rv	ggggggcacggttgatcagggcc
G29W	fw	gcggccctgatcccacgtgccccccag
	rv	ctggggggcacgtgggatcagggccgc
G29Y	fw	gcggccctgatcatacgtgccccccagc
	rv	gctggggggcacgtatgatcagggccgc
P89F	fw	cggtgaccgtcccagaaaaccgccacgatcaccac
	rv	gtggtgatcgtggcggttttctgggacggtcaccg
P89H	fw	cggtgaccgtcccaatgaaccgccacgatc
	rv	gatcgtggcggttcattgggacggtcaccg
P89I	fw	cggtgaccgtcccatataaccgccacgatcaccac
	rv	gtggtgatcgtggcggttatatgggacggtcaccg
P89L	fw	gtgaccgtcccacagaaccgccacgat
	rv	atcgtggcggttctgtgggacggtcac
P89M	fw	gaccgtcccacataaccgccacgatcaccacgt
	rv	acgtggtgatcgtggcggttatgtgggacggtc
P89N	fw	cggtgaccgtcccaattaaccgccacgatcaccac
	rv	gtggtgatcgtggcggttaattgggacggtcaccg
P89Q	fw	gtgaccgtcccactgaaccgccacgat
	rv	atcgtggcggttcagtgggacggtcac
P89S	fw	gaccgtcccacgaaaccgccacgatca
	rv	tgatcgtggcggtttcgtgggacggtc
P89V	fw	accgtcccacacaaccgccacgatcaccac
	rv	gtggtgatcgtggcggttgtgtgggacggt
P89W	fw	accgtcccaccaaaccgccacgatcaccac
	rv	gtggtgatcgtggcggtttggtgggacggt

P89Y	fw	cggtgaccgtcccaataaaccgccacgatcaccac
	rv	gtggtgatcgtggcggtttattgggacggtcaccg

Graphs of steady-state kinetic analysis of *Tfu*-FNO with varying concentrations of NCBs

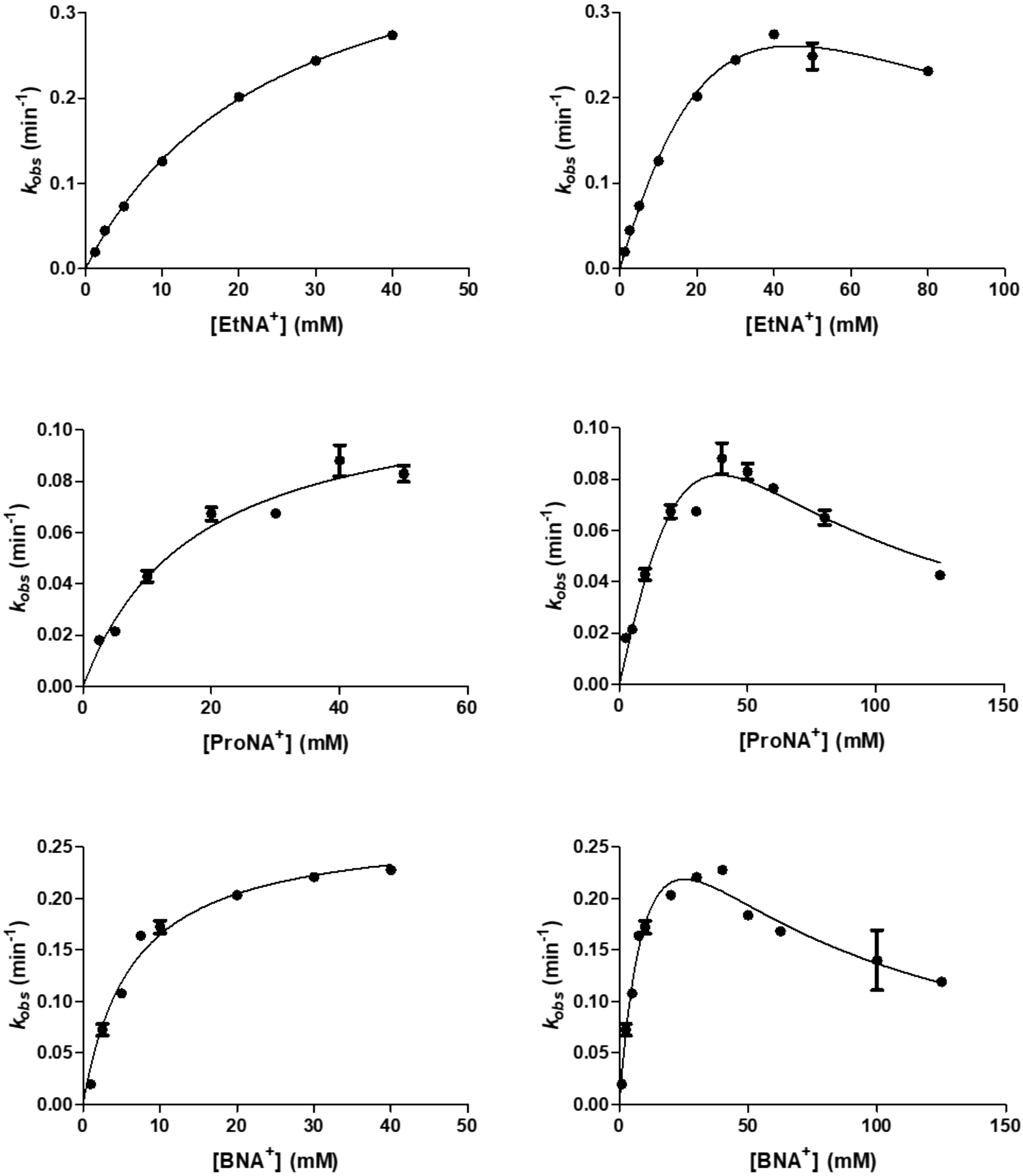

Figure S1: The observed initial rates, k_{obs}, of wild-type *Tfu*-FNO plotted against the concentrations of artificial nicotinamide cofactor biomimetics (NCBs) with apolar groups at position 1 of the nicotinamide. Data in the left column is fitted to the Michaelis-Menten formula and data in the right column is fitted to the Michaelis-Menten formula with substrate inhibition. Data was fitted by non-linear regression, GraphPad Prism v. 6.0 (GraphPad Software Inc., La Jolla, CA, U.S.A.). Data points and error bars represent means and standard deviations of triplicates, respectively. EtNA$^+$: 1-ethylnicotinamide, ProNA$^+$: 1-propylnicotinamide, BNA$^+$: 1-benzylnicotinamide.

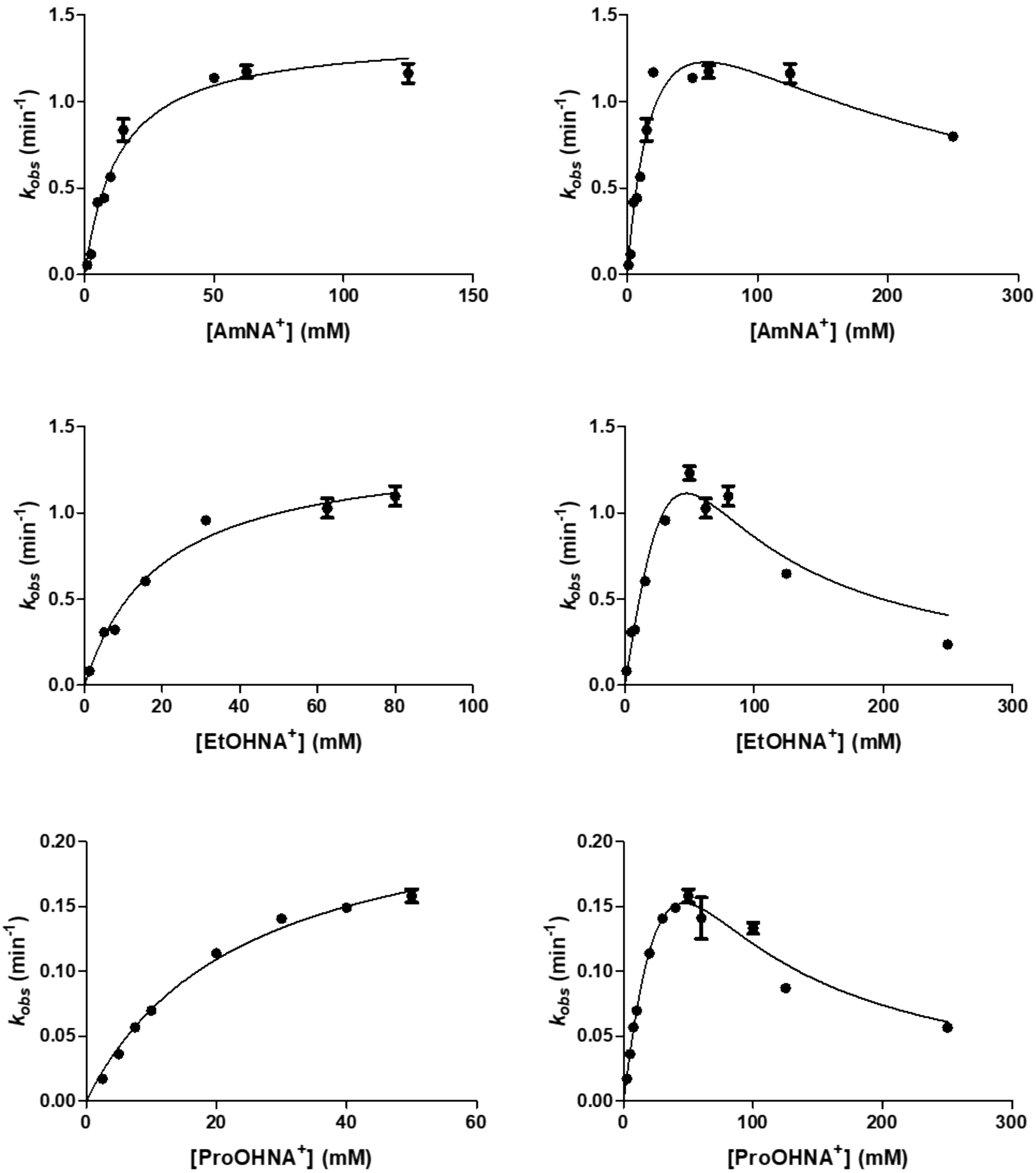

Figure S2: The observed initial rates, k_{obs}, of wild-type *Tfu*-FNO plotted against the concentrations of artificial nicotinamide cofactor biomimetics (NCBs) with polar groups at position 1 of the nicotinamide. Data in the left column is fitted to the Michaelis-Menten formula and data in the right column is fitted to the Michaelis-Menten formula with substrate inhibition. Data was fitted by non-linear regression, GraphPad Prism v. 6.0 (GraphPad Software Inc., La Jolla, CA, U.S.A.). Data points and error bars represent means and standard deviations of triplicates, respectively. EtOHNA$^+$: 1-hydroxyethylnicotinamide, ProNA$^+$: 1-hydroxypropylnicotinamide, AmNA$^+$: 1-carbamoylethylnicotinamide.

Activity screen for different *Tfu*-FNO mutants with selected NCBs

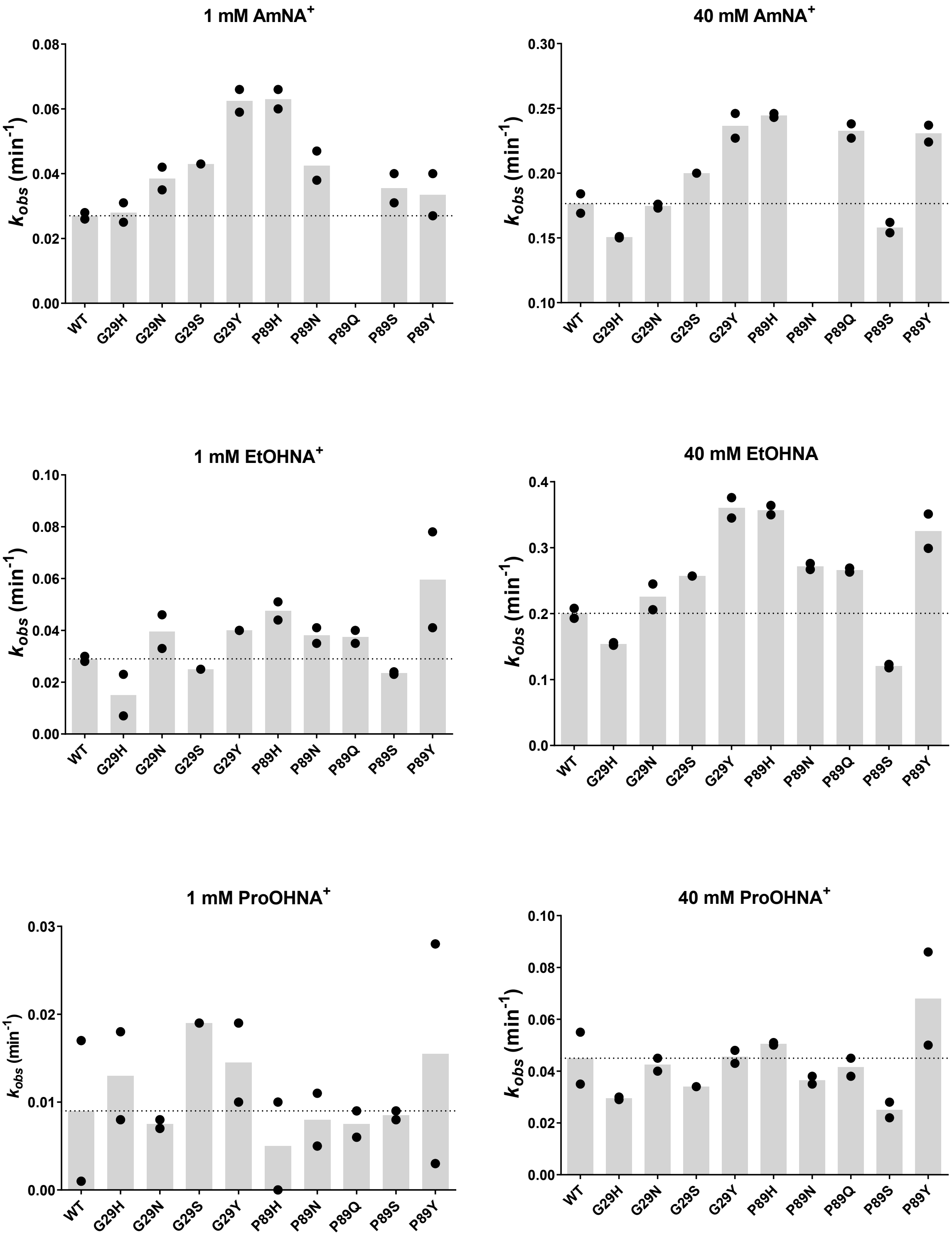

Figure S3: Activity screen of selected *Tfu*-FNO G29X and P89X variants with polar amino acid side chains toward artificial nicotinamide cofactor biomimetics (NCBs) with polar groups at position 1 of the nicotinamide. Data in the left column and right column are the activity measured with 1 mM NCB and 40 mM NCB, respectively. Data points represents individual k_{obs} measurements and bars represent the mean value of these two data points. The horizontal dotted line is the mean value of wild-type activity.

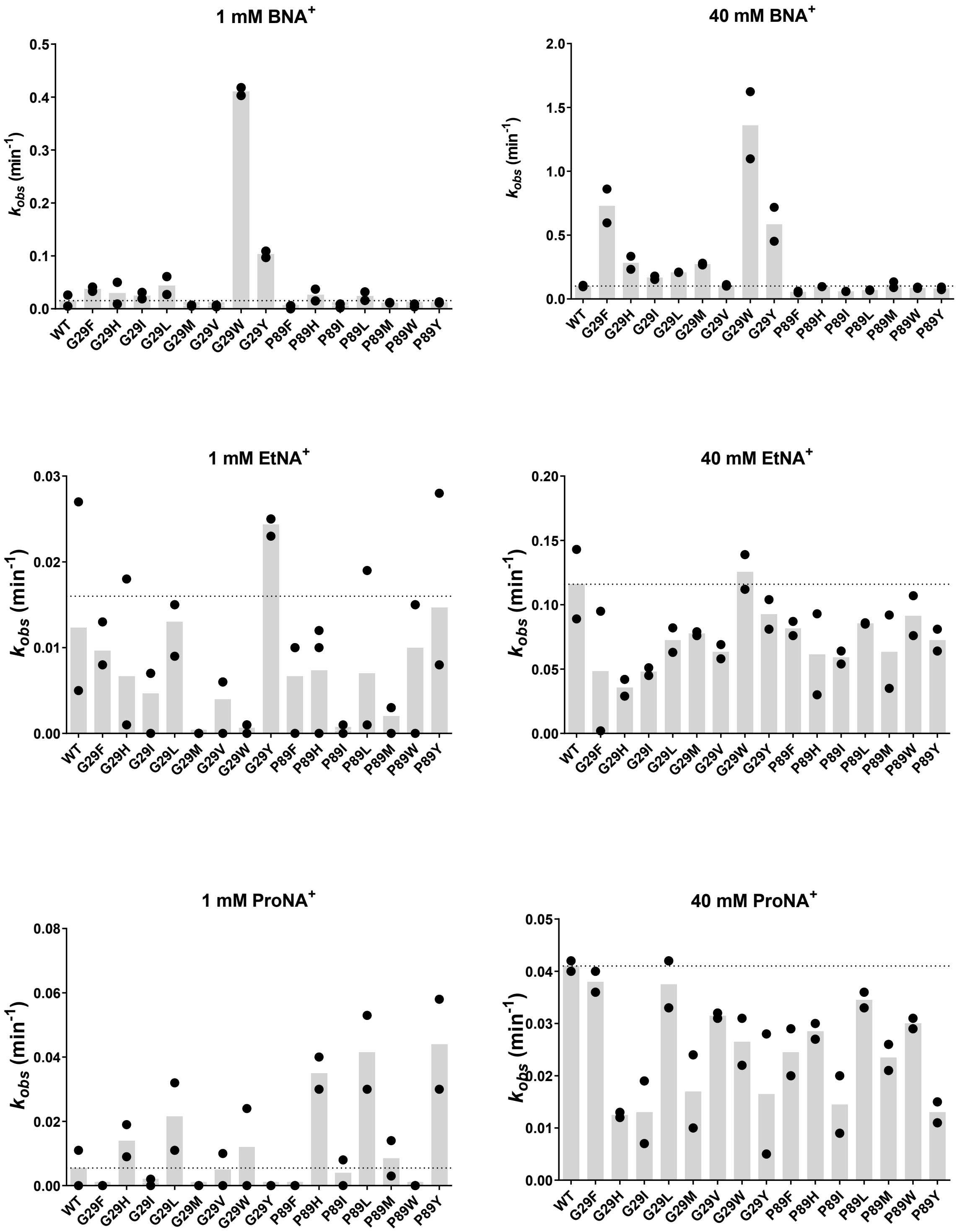

Figure S4: Activity screen of selected *Tfu*-FNO G29X and P89X variants with apolar amino acid side chains toward artificial nicotinamide cofactor biomimetics (NCBs) with apolar groups at position 1 of the nicotinamide. Data in the left column and right column are the activity measured with 1 mM NCB and 40 mM NCB, respectively. Data points represents individual k_{obs} measurements and bars represent the mean value of these two data points. The horizontal dotted line is the mean value of wild-type activity.

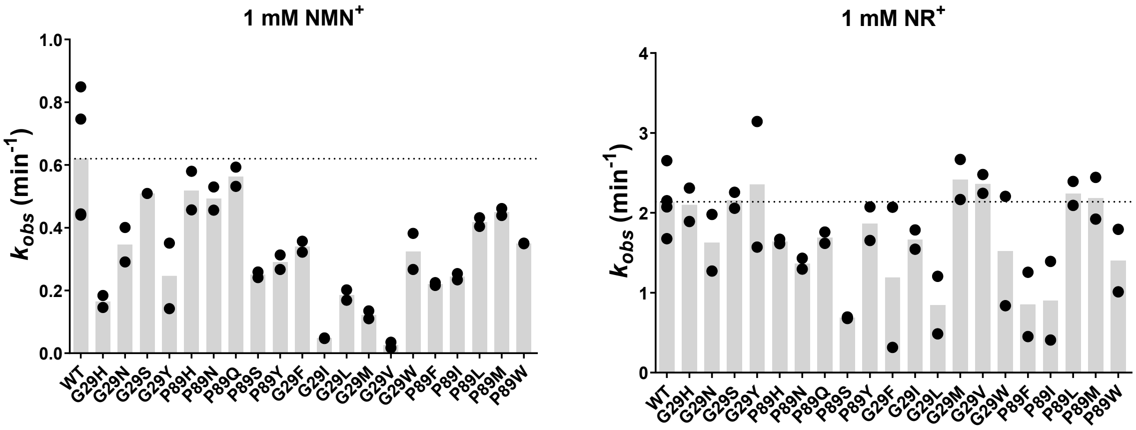

Figure S5: Activity screen of selected *Tfu*-FNO G29X and P89X variants toward the natural NAD(P) precursors nicotinamide ribose (NR) and nicotinamide mononucleotide (NMN). Data points represents individual k_{obs} measurements and bars represent the mean value of these two data points. The horizontal dotted line is the mean value of wild-type activity.

Graphs of steady-state kinetic analysis of engineered *Tfu*-FNO variants with varying concentrations of NCBs

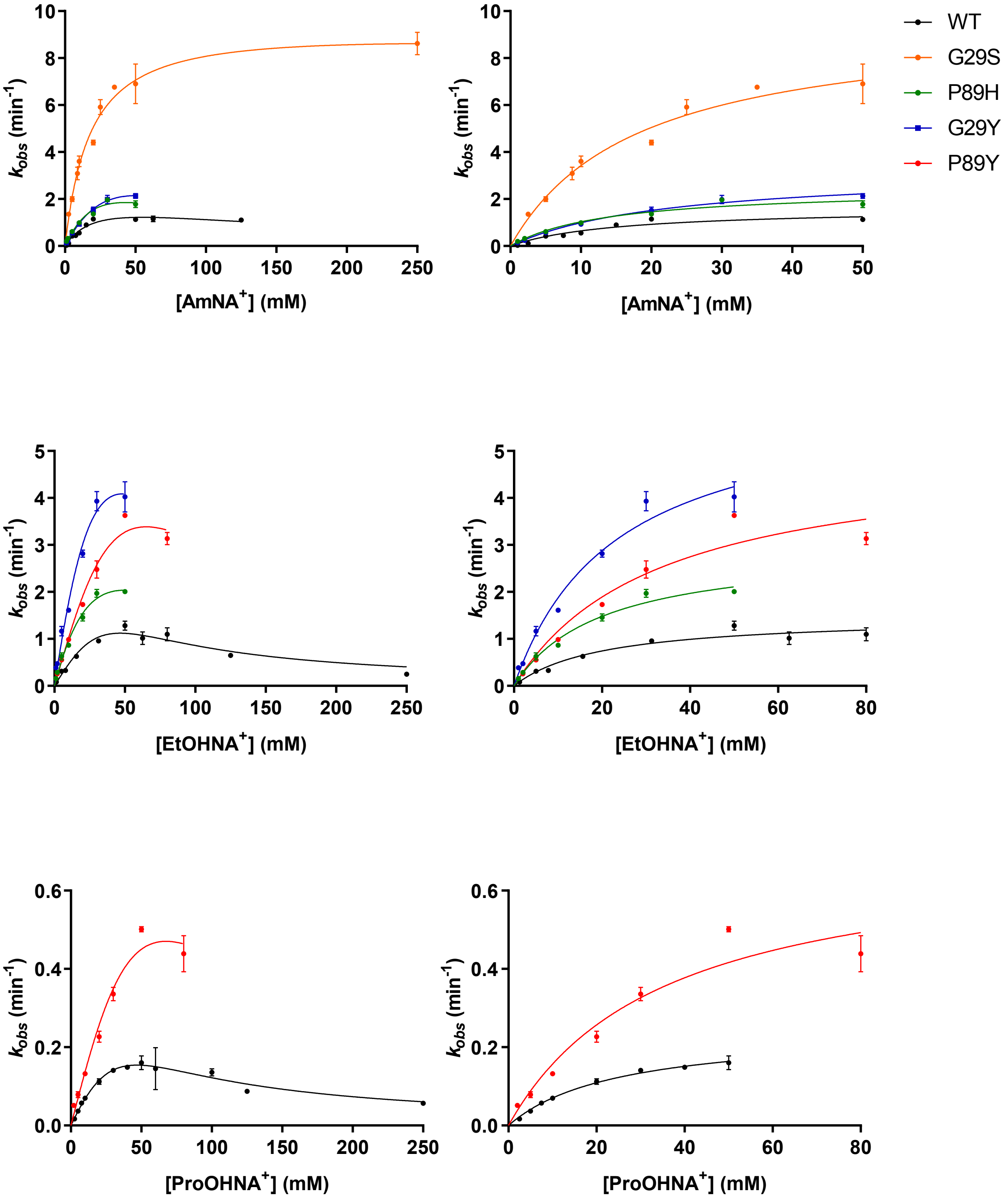

Figure S6: The observed initial rates, k_{obs}, of selected *Tfu*-FNO G29X and P89X variants with polar side chains plotted against the concentrations of artificial nicotinamide cofactor biomimetics (NCBs) with polar groups at position 1 of the nicotinamide. Data in the left column is fitted to the Michaelis-Menten formula with substrate inhibition and data in the right column is fitted to the Michaelis-Menten formula. Data was fitted by non-linear regression, GraphPad Prism v. 6.0 (GraphPad Software Inc., La Jolla, CA, U.S.A.). Data points and error bars represent means and standard deviations of triplicates, respectively. EtOHNA$^+$: 1-hydroxyethylnicotinamide, ProNA$^+$: 1-hydroxypropylnicotinamide, AmNA$^+$: 1-carbamoylethylnicotinamide.

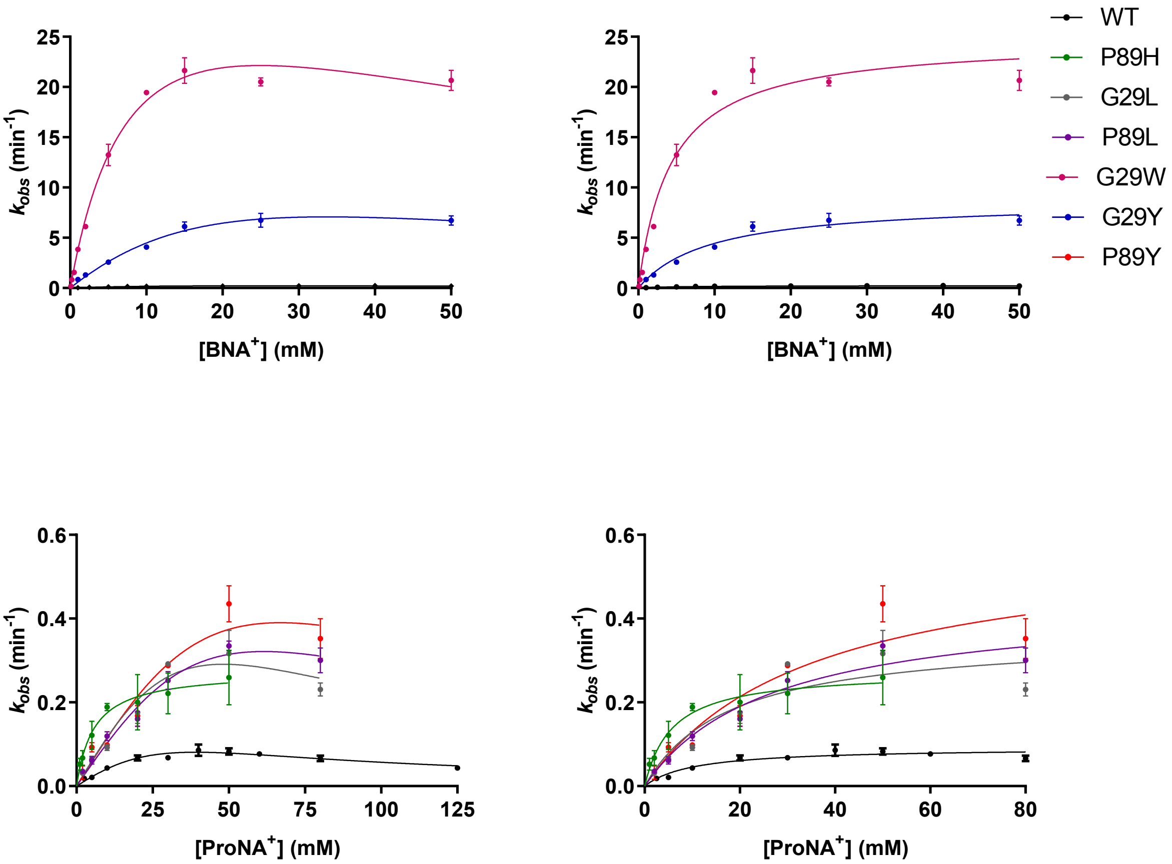

Figure S7: The observed initial rates, k_{obs}, of selected *Tfu*-FNO G29X and P89X variants plotted against the concentrations of artificial nicotinamide cofactor biomimetics (NCBs) with apolar groups at position 1 of the nicotinamide. Data in the left column is fitted to the Michaelis-Menten formula with substrate inhibition and data in the right column is fitted to the Michaelis-Menten. Data was fitted by non-linear regression, GraphPad Prism v. 6.0 (GraphPad Software Inc., La Jolla, CA, U.S.A.). Data points and error bars represent means and standard deviations of triplicates, respectively. EtNA$^+$: 1-ethylnicotinamide, ProNA$^+$: 1-propylnicotinamide, BNA$^+$: 1-benzylnicotinamide.

Activity screen for double mutants with selected NCBs

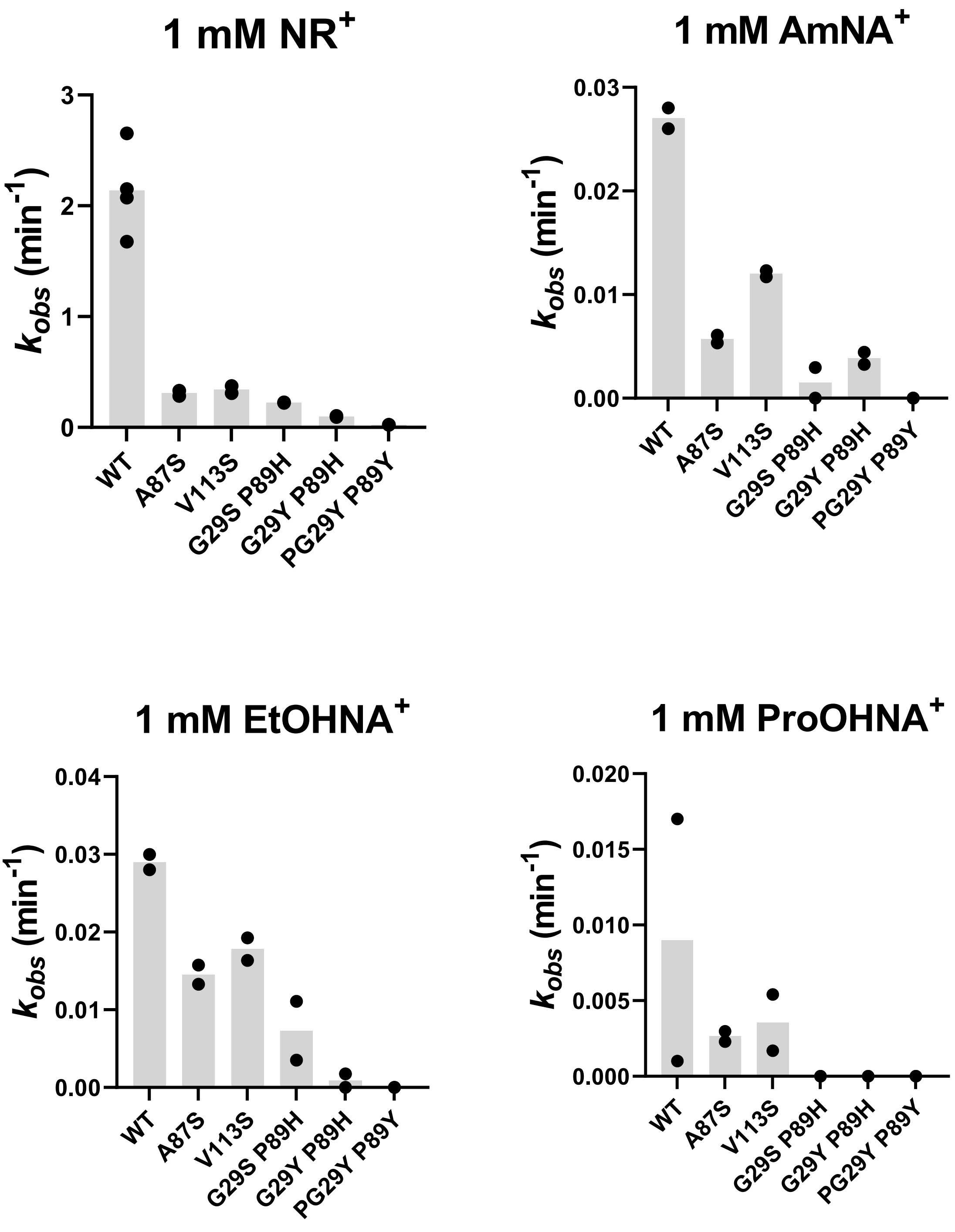

Figure S8: Activity screen of selected *Tfu*-FNO G29X/P89X double mutant variants, as well as A87S and V113S, toward the natural NAD(P) precursor nicotinamide ribose (NR) and the polar artificial nicotinamides $AmNA^+$, $EtOHNA^+$ and $ProOHNA^+$. Data points represent individual k_{obs} measurements and bars represent the mean value of these two data points.

pH dependence for NCB reduction by *Tfu*-FNO

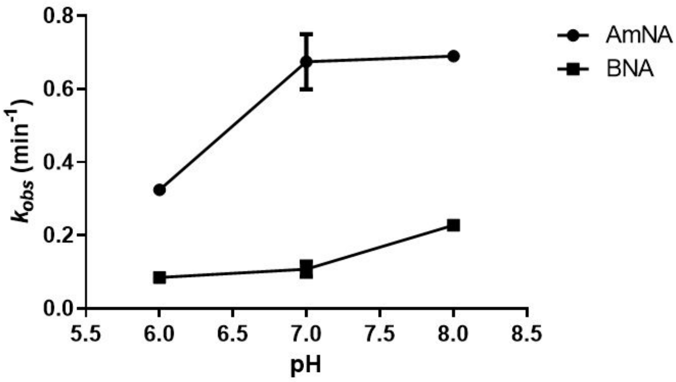

Figure S9: pH dependence of NCB-reduction by *Tfu*-FNO.

Steady-state kinetic parameters for *Tfu*-FNO variants toward selected $NADP^+$

Table S2: Steady-state kinetic parameters for wild-type *Tfu*-FNO and selected *Tfu*-FNO G29X and P89X variants toward selected $NADP^+$. Values are means from 3 independent measurements ± standard deviations.

variant	k_{cat} (s^{-1})		K_m (µM)		k_{cat}/K_m (s^{-1} M^{-1})		$(k_{cat}/K_m)_{mutant}$ /$(k_{cat}/K_m)_{wt}$	
wt	4.9	± 0.21	1.1	± 0.21	$4.5 \cdot 10^6$	$\pm 8.7 \cdot 10^5$		
G29L	0.63	± 0.03	$1.2 \cdot 10^3$	± 140	522	± 65	$1.2 \cdot 10^{-4}$	$\pm 2.7 \cdot 10^{-5}$
G29W	2.6	± 0.13	697	± 109	$3.7 \cdot 10^3$	± 612	$8.4 \cdot 10^{-4}$	$\pm 2.1 \cdot 10^{-4}$
G29Y	0.17	± 0.005	8.2	± 0.72	$2.1 \cdot 10^4$	$\pm 1.9 \cdot 10^3$	$4.7 \cdot 10^{-3}$	$\pm 1.0 \cdot 10^{-3}$
P89H	20	± 0.61	14	± 1.5	$1.4 \cdot 10^6$	$\pm 1.5 \cdot 10^5$	0.3	± 0.07
P89L	0.55	± 0.02	65	± 8.0	$8.4 \cdot 10^3$	$\pm 1.1 \cdot 10^3$	$1.9 \cdot 10^{-3}$	$\pm 4.4 \cdot 10^{-4}$
P89Y	3.9	± 0.16	86	± 15	$4.5 \cdot 10^4$	$\pm 8.1 \cdot 10^3$	$1.0 \cdot 10^{-2}$	$\pm 2.7 \cdot 10^{-3}$